Multichannel Equalization for High Track Density Magnetic Recording *

Mathew P. Vea
Digital Equipment Corp.
333 South St., M/S SHR 1-3/E29
Shrewsbury, MA 01545

José M.F. Moura
Electrical and Computer Engineering Dept.
Carnegie Mellon University
Pittsburgh, PA 15213-3890

Abstract

We have studied single and multiple channel equalization techniques for improving detection performance at high track densities. A multichannel matched filter approach is used to bound the performance gain that can be expected from an equalizer specifically designed to reduce intertrack interference. Side reading of the head is simulated at various off-track head positions using the reciprocity integral. Significant performance improvements are predicted for a three element head detecting data on the center track. Up to 2 dB improvement in SNR is predicted for the three element scheme while the head is on-track and up to 5 dB improvement as the head moves off track.

1 Introduction

Increased track density in a rigid disk drive implies decreased signal to noise ratio (SNR), increased interference from adjacent tracks, and more stringent track following requirements. Recent efforts have sought signal processing solutions that will allow higher track densities [1, 2, 3]. In this study, we evaluate and compare single and multichannel equalization approaches for reducing intertrack interference.

Application of signal processing to increase track density requires a clear understanding of the issues and good models of the physical processes involved. Figure 1 depicts the read process. The head, reading the center track, picks up interference from adjacent tracks and old information in the guard band due both to tracking error ϵ_{wr}, as it wanders from track center, and to side reading, as the head reads wider than its physical width.

We focus our study on intertrack interference by restricting our model to the multichannel equivalent of an isolated pulse, that is, a set of adjacent tracks with an isolated pulse on each track. We use a multichannel matched filter to reduce the channel to a discrete model, as described in Section 2. We derive equalizers for a single and multielement heads in Section 3. We use the reciprocity equation to simulate the side reading responses of different width heads. Finally, in Section 4 we compute the performance of equalizers for single and three element heads as a function of the off-track position of the head to estimate the potential performance gain of multielement heads.

*This material is based on work supported by the National Science Foundation under Grant No. ECD-8907068. The government has certain rights in this material.

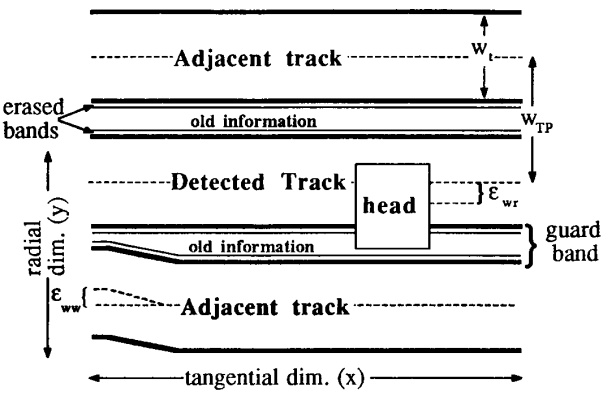

Figure 1: Read process geometry: looking down on the disk, the head reading the center track.

2 Multichannel Model

The multichannel model consists of K heads sensing L tracks, of which M are detected, as shown in Figure 2. Each head's response $x_i(t)$ is formed by the superposition of its responses to the data track and each of the interfering tracks, and includes additive white Gaussian noise:

$$x_k(t) = \sum_{i=1}^{L} p_{ik}(t)\theta_i + n_k(t). \quad (1)$$

The model is summarized in matrix notation:

$$\mathbf{x}(t) = \mathbf{P}^T(t)\Theta + \mathbf{n}(t), \quad (2)$$

where the individual head signals $\{x_i(t)\}$, the noise signals $\{n_i(t)\}$, and the data symbols $\{\theta_k\}$ are collected in vectors:

$$\mathbf{x}(t) = \begin{bmatrix} x_1(t) \\ x_2(t) \\ \vdots \\ x_K(t) \end{bmatrix}, \ \mathbf{n}(t) = \begin{bmatrix} n_1(t) \\ n_2(t) \\ \vdots \\ n_K(t) \end{bmatrix}, \ \Theta = \begin{bmatrix} \theta_1 \\ \theta_2 \\ \vdots \\ \theta_L \end{bmatrix}. \quad (3)$$

The pulse functions are similarly collected in the $(L \times K)$ matrix $\mathbf{P}(t)$, whose (l,k) element is $p_{lk}(t)$, the *pulse response* of head k to track l. The channel model consists of the set of pulses $\{p_{lk}(t)\}$ and the set of noise processes $\{n_l(t)\}$. Each of the pulse responses $p_{lk}(t)$ is mean square integrable:

$$\forall\{l,k\}: \quad \int_{-\infty}^{\infty} p_{lk}^2(t)dt < \infty. \quad (4)$$

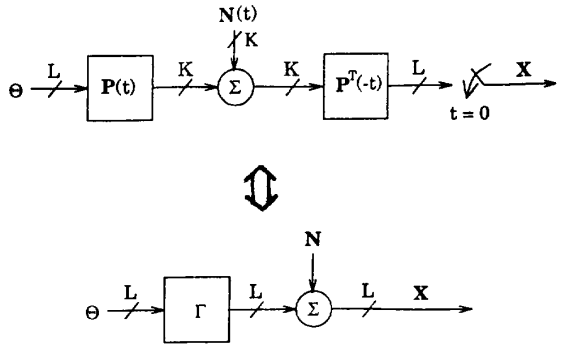

Figure 2: Equivalence of discrete time and continuous time multichannel models

The noises $\{n_i(t)\}$ are mutually independent zero mean white Gaussian processes, each with variance equal to σ^2. The data symbols are binary ($\theta_k \in \{-1, 1\}$) with equal probability. They are independent, so $E\{\Theta\Theta^T\} = I$. The noise processes and data symbols are independent of each other.

Van Etten has shown that the multichannel matched filter is a sufficient statistic for the detection of Θ[4]. As shown in Figure 2, the sufficient statistic $\mathbf{x}$ is formed by sampling the output of the multichannel matched filter $\mathbf{P}(-t)$ at $t = 0$:

$$\begin{aligned} \mathbf{x} &= \int_{-\infty}^{\infty} \mathbf{P}(t)\mathbf{x}(t)dt \\ &= \int_{-\infty}^{\infty} \mathbf{P}(t)\mathbf{P}^T(t)\Theta dt + \int_{-\infty}^{\infty} \mathbf{P}(t)\mathbf{n}(t)dt \\ &= \Gamma\Theta + \mathbf{n}. \end{aligned} \tag{5}$$

The matrix Γ is formed by taking the sum of inner products of each row of $\mathbf{P}^T(t)$ with each column of $\mathbf{P}(t)$:

$$\gamma_{ij} = \sum_{k=1}^{K} \langle p_{ik}(t), p_{jk}(t) \rangle_t , \tag{6}$$

where the inner product of two real functions $a(t)$, $b(t)$ is defined as:

$$\langle a(t), b(t) \rangle_t = \int_{-\infty}^{\infty} a(t)b(t)dt. \tag{7}$$

The noise vector $\mathbf{n}$ is similarly formed by taking sums of inner products of each row of $\mathbf{P}^T(t)$ with $\mathbf{n}(t)$:

$$n_i = \sum_{k=1}^{K} \langle p_{ik}(t), n_k(t) \rangle_t \tag{8}$$

The vector $\mathbf{n}$ is Gaussian with autocorrelation equal to $\sigma^2\Gamma$, as is easily verified. Because $\mathbf{x}$ is a sufficient statistic for the detection of Θ, the discrete time channel model represented by equation (5) is equivalent to the continuous time channel model of equation (1). The dimension of the sufficient statistic is L: the total number of tracks, both detected and interfering, that are present in the multichannel read signal $\mathbf{x}(t)$.

In our model, M of the L data symbols in Θ are detected. The symbols from the M data tracks are collected in vector Θ^d and the $L - M$ *nuisance* symbols are collected in vector Θ^n:

$$\Theta = \begin{bmatrix} \Theta^d \\ \Theta^n \end{bmatrix}. \tag{9}$$

3 Design of equalizers

The sufficient statistic $\mathbf{x}$, of dimension L, is useful for computing an upper limit on detector performance. In practice, the signals from the K heads are filtered by a linear multichannel equalizer whose output is of dimension M, the number of detected tracks. This operation is performed by a $(L \times M)$ weight matrix $\mathbf{W}$. The statistic $\mathbf{y}$ is therefore a linear combination of the sufficient statistic $\mathbf{x}$:

$$\mathbf{y} = \mathbf{W}^T\mathbf{x} = \mathbf{W}^T\Gamma\Theta + \mathbf{W}^T\mathbf{n} \tag{10}$$

As an aside, it is not necessary to implement the full multichannel matched filter if the dimension of the equalizer output is less than L. Instead, the multichannel matched filter $\mathbf{P}(-t)$ and the linear equalizer $\mathbf{W}$ will be combined into the single multichannel equalizer represented by the $(M \times K)$ matrix of pulse functions $\mathbf{W}^T\mathbf{P}(-t)$:

$$\mathbf{y} = \mathbf{W}^T \int_{-\infty}^{-\infty} \mathbf{P}(t)\mathbf{x}(t)dt = \int_{-\infty}^{-\infty} \left(\mathbf{W}^T\mathbf{P}(t)\right)\mathbf{x}(t)dt. \tag{11}$$

Minimum probability of error equalizer

The ideal equalizer is one that minimizes the probability of detector error ($P(e)$). The equalizer weight ($\mathbf{W}$) that minimizes $P(e)$ is easily determined when $P(e)$ is expressed as a function of $\mathbf{W}$. If each track is detected separately using a single element of y, the multichannel weight matrix $\mathbf{W}$ can be partitioned into M weight vectors $\{\mathbf{w}_i\}$:

$$\mathbf{W}^T = \begin{bmatrix} \mathbf{w}_1^T \\ \vdots \\ \mathbf{w}_M^T \end{bmatrix}. \tag{12}$$

Each weight vector $\mathbf{w}_i$ is selected to optimize the detection of desired symbol θ_i^d:

$$y_i = \mathbf{w}_i^T\mathbf{x} = \mathbf{w}_i^T\Gamma\Theta + \mathbf{w}_i^T\mathbf{n}. \tag{13}$$

The detector compares y_i to a threshold. For the case of equally probable binary data symbols ($\theta_i \in \{-1, 1\}$) in white Gaussian noise, this threshold is at $y_i = 0$ [5]. The $P(e)$ in detecting symbol θ_i^d is therefore simply the sum of the probabilities of error conditioned on all possible values of the other $(L - 1)$ symbols. Because y_i is Gaussian conditioned on Θ, this expression reduces to a sum of error functions:

$$\begin{aligned} P(e) &= \sum_{j=1}^{2^{L-1}} P(e|\Theta_j)P(\Theta_j) \\ &= \frac{1}{2^{(L-1)}} \sum_{j=1}^{2^{L-1}} Q\left(\frac{\mathbf{w}^T\Gamma\Theta_j}{\sigma\sqrt{\mathbf{w}^T\Gamma\mathbf{w}}}\right) \end{aligned} \tag{14}$$

Parameter	*Symbol*
Head-Medium separation	d
Medium thickness	δ
Full track width	w_t
Width of erased band	w_e
Head gap	g
Length of flux reversal	a_x
Velocity	V
Bit detection window	T
Track pitch	w_{tp}

Table 1: Physical parameters used in simulation

where $Q(x)$ is a complementary error function:

$$Q(x) = \frac{1}{\sqrt{2\pi}} \int_x^\infty e^{-y^2/2} dy. \tag{15}$$

The minimum probability of error (MPE) equalizer is simply the weight vector w that minimizes the expression for $P(e)$ in equation (14). This optimum weight vector can be found by standard numerical optimization methods.

Naive equalizer

We will evaluate the performance of the MPE equalizer in comparison to the *naive* single channel equalizer, which we define as the equalizer whose response is matched to the on-track pulse response of the channel. Specifically, when the i^{th} track is the data track, the naive equalizer weight vector is equal to the i^{th} elementary vector:

$$\mathbf{w}^T = \mathbf{e}_i = [\ 0 \quad \cdots \quad 0 \quad 1 \quad 0 \quad \cdots \quad 0\ ] \tag{16}$$

This is the best equalizer in the absence of knowledge about intertrack interference, and so it serves as a good baseline for comparison of equalizer designs.

4 Simulation and Results

To generate simulations for the comparison of the equalizers, we used a previously described model[6] to to compute Γ for different head geometries. This model numerically integrates the reciprocity equation to compute pulse shapes as a function of off-track position of the head for a given track geometry. We used an arctangent function to represent the flux transition magnetization pattern, and we used an expression derived by Lindholm[7] to describe the three dimensional head field. We then simulated the responses of three different width heads, computing the inner product matrix Γ for each head at several off-track positions. The parameter values used in the simulations were: $a_x/(VT) = 1.5$, $a_x/g = 0.5$, $w_t/w_h = 1.1$, $w_{tp}/w_h = 1.4$, $w_e/w_t = .05$, $d/\delta = 5$, $d/g = 0.5$, and $w_h/d = 11, 20, 30$, where the parameters are defined in Table 1. To compare the different width heads, we assumed that the SNR scaled as the square root of the head width, but otherwise the value of the noise variance σ^2 was arbitrarily chosen.

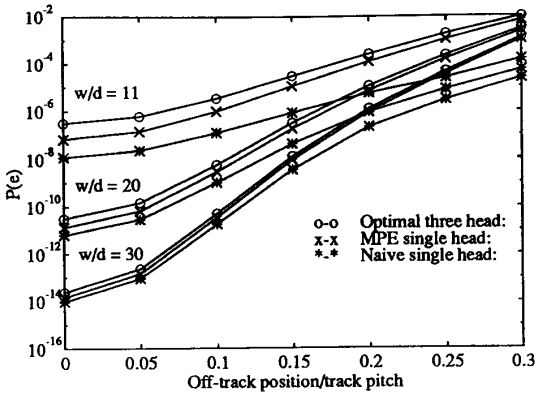

Figure 3: Bathtub performance curves

We compared three different widths of heads, as characterized by the ratio w_h/d. The ratios in our simulations represent very narrow heads, and were chosen to study the effectiveness of equalization in the presence of high levels of intertrack interference. We simulated both a single head and a three element head reading a single track, corresponding to (K, L, M) values of (1,5,1) and (3,9,1), respectively. The intertrack interference included adjacent tracks and old information "tracks" from both sides of the head. For the multielement read head, we assumed that each element was centered on one of the three tracks and that the elements had identical side reading parameters.

We then computed the probability of error using equation (14) for the computed Γ matrices. The performances of single head MPE, single head naive, and three element head MPE equalizers were computed for each of the different width heads. The resulting plots of probability of error vs. off-track head position, known as "bathtub" curves, are shown in Figure 3. The head position is normalized by the track pitch, so that scaling on the bathtub curves is different for the different width heads.

For each of the three heads, the single channel minimum probability of error (MPE) equalizer outperforms the naive equalizer, and the three channel MPE equalizer outperforms both of the single channel equalizers for all off-track values, as is clear in Figure 3. It is also clear the SNR penalty for decreasing the head width is a larger than any gains in equalizer performance due to increased side reading. It is also true, but less clear in this figure, that the gain in equalization performance of the single and three channel MPE equalizers is larger for a narrow head than a wide head. Furthermore, the "bathtub" of the three channel equalizer flattens out somewhat at large off-track values. These effects can be seen more clearly if the performance of the MPE equalizers are plotted relative to the naive equalizer performance.

In order to directly compare the performance of these three detectors we define the inverse Q function such that:

$$Q^{-1}(Q(x)) = x, \tag{17}$$

where Q(x) is defined in Equation (15). The inverse exists because Q is a monotonic function over the positive real numbers. Then, since the argument of Q corresponds to the SNR

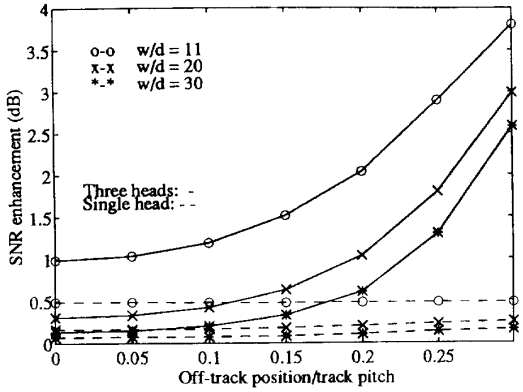

Figure 4: SNR improvement for single and three head equalizers

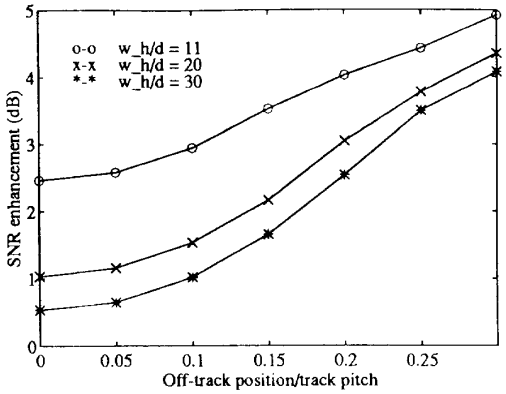

Figure 5: SNR improvement for case without guard band

of the channel, and since the $P(e)$ can be coarsely modeled as the output of an error function, we define the signal to noise ratio gain of $P_1(e)$ relative to $P_2(e)$ as:

$$SNR_{P_1/P_2} = 20\log_{10}\frac{Q^{-1}(P_1(e))}{Q^{-1}(P_2(e))} \tag{18}$$

We have plotted the SNR gains of the single and the three channel MPE equalizers relative to the naive equalizer using the same data shown in Figure 3. The results are shown in Figure 4. It is clear from this figure that the MPE performance gains increase as the head becomes narrower. This trend is due to the increased side reading of the narrower heads and the relative improvement of the MPE equalizers in the presence of higher levels of intertrack interference. Furthermore, the relative gain of the three channel MPE equalizer increases dramatically as the head moves off-track, while the performance gain of the single channel MPE equalizer is flat.

The improved performance of the three channel equalizer in the presence of higher interference levels suggests that a multihead system may require less of a guard band. We therefore conducted a second simulation using the same parameters as those used to generate Figures 3 and 4 except track pitch, which was set to $w_{tp}/w_h = 1.15$. This track pitch corresponds to the case where the erased bands of adjacent tracks exactly overlap and the old information in the guard band is completely erased. The SNR gains of the three channel head were plotted again and the results are shown in Figure 5. The difference between the performance gains for the three element head with and without a guard band are particularly significant when the head is on-track or when its off-track error is small. Thus, multichannel equalization promises increased track density through both decreased track width and decreased guard band width. However, determination of the optimum guard band width requires a stochastic simulation incorporating both write and read misregistration[8].

Performance Within Parameter Space

In order to determine the generality of the above multichannel simultion results, we examined equalizer performance over the entire parameter space of two simple channel models. The first channel consists of a single track with a single interfering track[5]. The second channel consists of two symmetrically cross-coupled channels[1]. To some extent, these two simple models approximate the cases where one interference source is dominant, for a single head and for multielement heads, respectively. Each of these two examples can be described with just two parameters, γ and ρ, which correspond with the amplitude of the intertrack interference and its correlation with the on-track channel response.

Each of the examples can be described with the multichannel model of equation (2). The pulse matrix $\mathbf{P}(t)$ and channel matrix Γ for the single channel example are:

$$\mathbf{P}(t) = \begin{bmatrix} p_1(t) \\ p_2(t) \end{bmatrix}, \quad \Gamma = \begin{bmatrix} 1 & \gamma\rho \\ \gamma\rho & \rho^2 \end{bmatrix}. \tag{19}$$

Here $p_1(t)$ is the on-track pulse response and $p_2(t)$ is the cross-track pulse response. For convenience the amplitude of $p_1(t)$ is assumed to be equal to 1. The parameter ρ is the relative amplitude of the intertrack interference, while γ is the correlation between the on-track and intertrack pulse responses:

$$\rho = \sqrt{\langle p_2(t), p_2(t)\rangle_t} = \|p_2(t)\|, \quad \gamma = \frac{\langle p_1(t), p_2(t)\rangle_t}{\|p_2(t)\|}. \tag{20}$$

The optimal performance gain, defined using equation (18) as the SNR gain of the MPE detector relative to the naive equalizer, has been computed for a mesh of ρ and γ values. The contour plot of the SNR gain, measured in decibels, is shown in Figure 6. We also computed the values of ρ and γ for the largest amplitude interfering track of the three heads from the previous simulation at head positions from zero to 30% off-track. A trace of each of these three curves is overlaid onto the contour plot. Not surprisingly, both the amplitude and the correlation with the data pulse increase for the interfering pulse as the head moves off track. Looking closely at this contour plot, it is clear why the single channel equalizer is unable to improve performance more than a few

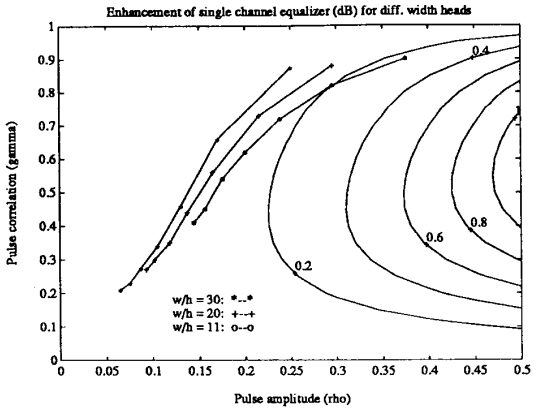

Figure 6: Contour plot of single channel, single interfering pulse case

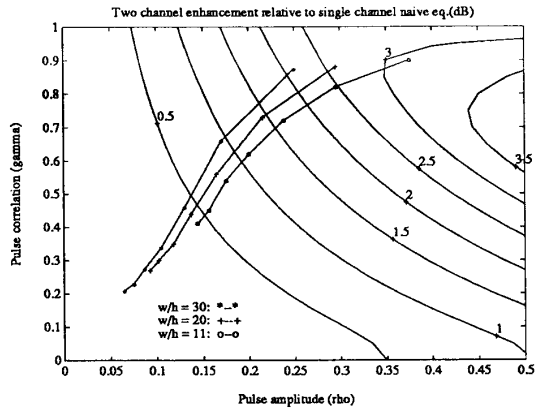

Figure 7: Contour plot of symmetrically coupled two channel case

tenths of a dB. The single channel equalizer works best if the amplitude of the interference is high and the interference is moderately correlated with the data signal. Unfortunately, for an adjacent track to be large in amplitude, the head must be directly reading (not side reading) the adjacent track. In this case, the response of the head resembles the response of the head to the data track, and the equalizer is unable to distinguish signal from interference.

The pulse matrix $\mathbf{P}(t)$ and the channel matrix for the two channel example are:

$$\mathbf{P}(t) = \begin{bmatrix} p_1(t) & p_2(t) \\ p_2(t) & p_1(t) \end{bmatrix}, \quad \Gamma = \begin{bmatrix} 1+\rho^2 & 2\gamma\rho \\ 2\gamma\rho & 1+\rho^2 \end{bmatrix}, \quad (21)$$

where $p_1(t)$ is the on-track pulse response, $p_2(t)$ is the cross-track pulse response, and ρ and γ are defined by equation (20). Again, the contour plot of the two channel equalizer performance gain relative to the single channel naive equalizer is plotted in Figure 7, and the traces of the parameter values for the adjacent track representing the largest interference are overlaid over the contours. As shown, the two channel equalizer promises significant performance improvement, increasing as the head moves off track. It is clear from Figures 6 and 7 that multichannel equalizers offer much more chance for decreasing intertrack interference than do single channel equalizers. Note also that the multichannel equalizer performance is less sensitive to pulse correlation ρ than the single channel example. This is because the multichannel equalizer operates mainly by *canceling* the interference while the single channel equalizer operates by filtering the interference.

5 Conclusions

The results of our study indicate that significant performance gains can be achieved by using a three element read head and multichannel equalization to detect a single track. Furthermore, these are gains that cannot be matched using only a single head. For the most narrow heads considered, we predict up to 2 dB improvement in SNR while the head is on-track increasing to 5 dB improvement as the head moves far off-track. Because SNR increases with the square root of the track pitch, this improvement translates to almost a two-fold increase in track density, depending on the tracking error statistics. The multichannel equalizer cancels intertrack interference in the center head using the signals from the side heads to achieve its performance gain. A single channel equalizer operating on a signal from a single head must rely solely on spectral differences between the desired signal and the interference to filter out the interference. A future study that incorporates track writing error as well as track reading error is planned. This study will yield a better prediction of the track density increase obtainable from three element read heads.

References

[1] L. C. Barbosa, "Simultaneous detection of readback signals from interfering magnetic recording tracks using array heads," *IEEE Trans. on Magnetics*, vol. 26, pp. 2163–2165, Sept. 1990.

[2] W. L. Abbott, J. M. Cioffi, and H. K. Thapar, "Performance of digital magnetic recording with equalization and offtrack interference," *IEEE Trans. on Magnetics*, vol. 27, pp. 705–716, Jan. 1991.

[3] P. A. Voois and J. M. Cioffi, "Multichannel digital magnetic recording," in *ICC '92 Conference Record*, IEEE, May 1992.

[4] W. Van Etten, "Maximum likelihood receiver for multiple channel transmission systems," *IEEE Trans. on Communications*, vol. 24, pp. 276–283, Feb. 1976.

[5] M. P. Vea and J. M. F. Moura, "Detection in magnetic recording with cross-track interference," in *Conference Record of 25th Asilomar Conf. on Signals, Systems and Computers*, IEEE Computer Society Press, Nov. 1991, pp. 25–29.

[6] M. P. Vea and J. M. F. Moura, "Magnetic recording channel model with intertrack interference," *IEEE Trans. on Magnetics*, vol. 27, pp. 4834–4836, Nov. 1991.

[7] D. A. Lindholm, "Magnetic fields of finite track width heads," *IEEE Trans. on Magnetics*, vol. 13, pp. 1460–1462, Sep. 1977.

[8] M. P. Vea, *Intertrack Interference in High Density Recording: Modeling and Equalization*. PhD thesis, Carnegie Mellon University, Nov. 1993.